Exploring the potential pathogenic mechanism of Alzheimer's disease through in silico analysis of gamma secretase

Visentin, David

UNIVERSITY OF RIJEKA
DEPARTMENT OF BIOTECHNOLOGY
Graduate programme
"Medicinal chemistry"

David Visentin

Exploring the potential pathogenic mechanism of Alzheimer’s disease through in silico analysis of gamma secretase

Master's thesis

Rijeka 2021

UNIVERSITY OF RIJEKA
DEPARTMENT OF BIOTECHNOLOGY
Graduate programme
"Medicinal chemistry"

David Visentin

Exploring the potential pathogenic mechanism of Alzheimer’s disease through in silico analysis of gamma secretase

Master's thesis

Rijeka 2021

Mentor: Željko M. Svedružić, PhD, assistant professor

SVEUČILIŠTE U RIJECI

ODJEL ZA BIOTEHNOLOGIJU

Diplomski sveučilišni studij

"Medicinska kemija"

David Visentin

Istraživanje potencijalnih patogenih mehanizama Alzheimerove bolesti preko analize gama sekretaze

Diplomski rad

Rijeka 2021

Mentor rada: dr.sc. Željko M. Svedružić, docent

The thesis was defended on _____ in front of a committee:

1. _____

2. _____

3. _____

The thesis has ____ pages, ____ figures, ____ tables and ____ citations.

Summary

***Background**:* Alzheimer`s disease (AD) is a progressive neurologic disorder that causes brain atrophy and neuronal cell death which in turn manifests as dementia. In later stages of the disease patients are unable to care for themselves. This alongside the high number of people affected, makes AD the most expensive condition for health care providers in the industrialized nations. The pathogenic processes underlining AD usually occur through dysregulation of amyloid-β (Aβ) processing. The transmembrane protease responsible for Aβ cleavage is Gamma-secretase. All current attempts to cure AD trough regulation of γ-secretase have resulted in little to no observed effect on the pathogenesis of the disease. This miss in drug creation is caused by a lack of information regarding understanding Aβ formation. Better knowledge of the factors involved in Aβ processing is needed.

***Experimental**:* Gamma-secretase structures at 3.4 angstrom resolution were analyzed using multiscale molecular dynamic approaches and electrostatic calculations.

Results: Multiscale molecular dynamics can describe structural interactions that occur in the binding of C99-CTFβ to the γ-secretase complex. C99-CTFβ is capable of docking near the active site disrupting substrate processing. Such interactions can partially or fully inhibit gamma-secretase or shift the proteolytic cleavages from the Aβ 40 path to the neurotoxic Aβ 42. Nicastrine can exist in an open or a closed form. The closed form prevents substrates from interacting, preventing the disruption of the active site.

***Conclusion**:* Through substrate oversaturation, interactions can lead to a change in the mechanism and precision of Aβ cleavage. This can drive pathogenic processes in AD.

Keywords: Alzheimer's disease, γ-secretase, Amyloid-β, Molecular dynamics, Substrate docking

Sažetak

Pozadina: Alzheimerova bolest (AD) je progresivni neurološki poremećaj koji uzrokuje atrofiju mozga i smrt neuronskih stanica što se zauzvrat očituje kao demencija. U kasnijim fazama bolesti, pacijenti nisu u stanju brinuti sami za sebe. To zajedno s velikim brojem pogođenih ljudi, čini AD najskupljom bolesti za zdravstveni sektor u industrijaliziranim zemljama. Patogeni procesi koji dovode do bolesti obično se postižu poremećajem u regulaciji procesiranja amiloidnog proteina (Aβ). Transmembranska proteaza zaslužna za sječenje amiloida je γ-sekretaza. Svi pokušaji izlječenja AD preko regulacije γ-sekretaze su završili bezuspješno. Vjerojatni razlog tome je manjak razumijevanja mehanizma procesiranja amiloidnog proteina. Potrebni je više znanja o faktorima koji su uključeni u taj proces.

Eksperimentalno: Strukture gama-sekretaze, s razlučivošću od 3,4 Å, analizirane su korištenjem različitih molekularno-dinamičkih pristupa i elektrostatskih proračuna.

Rezultati: Molekularna dinamika može opisati strukturne interakcije koje se javljaju vezanjem C99-CTFβ na kompleks gama-sekretaze. C99-CTFβ se može dokirati u blizini aktivnog mjesta i time ometat procesiranje supstrata. Takve interakcije mogu djelomično inhibirati gama-sekretazu ili preusmjeriti proteolitičko cijepanje s Aβ 40 fragmenta na neurotoksični Aβ 42. Nikastrin može postojati u otvorenom ili zatvorenom obliku. Zatvoreni oblik onemogućava interakcije sa supstratom i time sprečava disrupciju aktivnog mjesta.

Zaključak: Preko zasićenja supstratom, moguće je dovesti do promjene u procesiranju amiloidnog proteina. Takve promjene mogu potaknuti nastanak Alzheimerove bolesti.

Ključne riječi: Alzheimerova bolest, Gama-sekretaza, Amiloid-β, Molekularna dinamika, Dokiranje supstrata

Abbreviations	Explanations
AD	Alzheimer’s disease
FAD	Familial Alzheimer’s disease
Aβ	Amyloid β
APP	Amyloid precursor protein
TM	Transmembrane domain
CTF	Carboxyl-terminal fragment
BACE1	β-site APP cleaving enzyme
NIC	Nicastrine
PSEN	Presenilin
APH1	Anterior pharynx-defective 1
PEN2	Presenilin enhancer protein 2
AICD	APP intracellular domain

Contents

1. Introduction

AD is a progressive and irreversible neurodegenerative disorder that slowly diminishes memory and thinking skills. Early symptoms are nonspecific and can vary, making the disease difficult to diagnose. They usually take the form of mild cognitive impairment focusing on the non-memory aspect of cognition. As the disease advances, it leads to progressive dementia with insidious onset of agnosia, aphasia, and apraxia. When nearing the end stages, it inhibits the ability of the patient to perform the simplest of tasks, resulting in a complete loss of ability for a person to care for themself [1]. Its main pathological features are cerebral atrophy, amyloid plaques, neurofibrillary tangles and a loss of connectivity between neurons in the brains of patients [2,3].

AD affects 6.2 million people in America and over 10 million in Europe. It is one of the most financially burdening diseases in the world. Alongside other forms of dementia, it reached a combined cost of over 600 billion dollars per year. This number is expected to surpass 1 trillion in America alone by 2050, with similar estimates being made for Europe. In the past two decades, incidence rose by 145% with two thirds of the affected being women [4,5].

There are two basic types of AD: sporadic and familial. Sporadic is a form of AD with late onset, no known cause, and no obvious inheritance pattern. On the other hand, familial Alzheimer's disease (FAD) is inherited within families. Characterized by an early onset and caused by genetic factors it affects less than 10 percent of AD patients. FAD gives crucial insight in the mechanism of AD [6].

In addition to genetics, some common risk factors include old age, stroke, diabetes and depression [6].

1.1. Mechanism of AD

In 1906, Alois Alzheimer presented the first case of AD in the world where he described changes in the tissue of a woman who has died due to an unusual mental illness [3]. The changes were later identified to be a combination of amyloid plaques and tau tangles. This phenotype became a main indicator of AD and at the same time, the center point for trying to determine a cure. Two main theories were formed, the amyloid hypothesis and the tau propagation hypothesis. After significant effort, due to lack of results, multiple other theories were formed. Some of which are cholinergic hypothesis, mitochondrial cascade hypothesis, calcium homeostasis hypothesis, inflammatory hypothesis, neurovascular hypothesis and metal ion hypothesis [2].

To this day, a mechanism that can explain the pathogenesis of AD has yet to be discovered. All current theories are unable to exactly predict and explain the observed phenotypes. This is one of the reasons why identifying a cure for AD has proven to be difficult [2].

1.2. Amyloid hypothesis

The amyloid hypothesis revolves around the Aβ peptide, citing it as the primary cause of AD. The idea was first proposed in 1991 by John Hardy and David Allsop. It was shown that in high concentrations, Aβ peptide has a neurotoxic effect on mature neurons. This was observed in the form of dendritic and axonal atrophy followed by neuronal death [2].

In the brain, Aβ exists in multiple forms: freely dissociated in solution, as an oligomer complex and as plaques. Different forms of Aβ trigger tau dissociation from the axons. This in turn diminishes neuronal interactions causing neuron death when combined with Aβ neurotoxicity [7].

Plaques are largely composed of Aβ protein aggregates that have increased longevity, stability, and consequent toxicity. Longevity of the plaques is derived from the β-sheet secondary structure that is difficult to degrade through normal microglial clearance processes [8].

By analyzing the brains of deceased patients with and without AD, it was observed that plaques do not necessarily contribute to the pathogenesis of AD. From this, it was concluded that other forms (notably oligomers) impact pathogenesis [9]. Further research also revealed that the important factor in AD formation is the ratio of different sized Aβ fragments, rather than its overall concentration [8].

Aβ is the result of enzymatic cleavage of amyloid precursor protein (APP). The main enzymes involved in the processing of APP are α-, β-, and γ-secretase [10].

While the function of APP in AD has been thoroughly explored in recent decades, its biological function is still poorly understood. While it is known that APP has no enzymatic activity, research indicates it may play a role in the regulation of biological processes that range from transcriptional regulation to synaptic functions. APP can function as a cell surface receptor-like protein or as a ligand, thus impacting cell biology. It can act either from the cell membrane or through its secreted proteolytic fragments, notably, APPsα which seems to have a neuroprotective function [11,12].

1.3. Amyloid processing

APP is a type-I transmembrane protein from the family of amyloid-like proteins. It has a conserved structure consisting of a single transmembrane domain (TM). APP undergoes complex proteolytic processing which yield biologically active fragments that have specific and sometimes even opposing functions [12].

There are two main pathways in the processing of APP, the anti-amyloidogenic and the amyloidogenic (Fig 1). Which pathway the protein will take depends on the interaction of three previously mentioned proteins α-, β-, and γ-secretase. Their names were given based on APP cleavage sites, cleaving at the alpha, beta, and gamma sites, respectively. Processing starts by cleaving of the most of the extracellular domain of APP by either alpha or β-secretase. This yields a large soluble APP derivative (called APPsα and APPsβ) and membrane-tethered α- or β-carboxyl-terminal fragment (APP-CTFα and APP-CTFβ). Newly formed CTFs is then further cleaved by γ-secretase while APPsα and APPsβ dissociate into extracellular space [8].

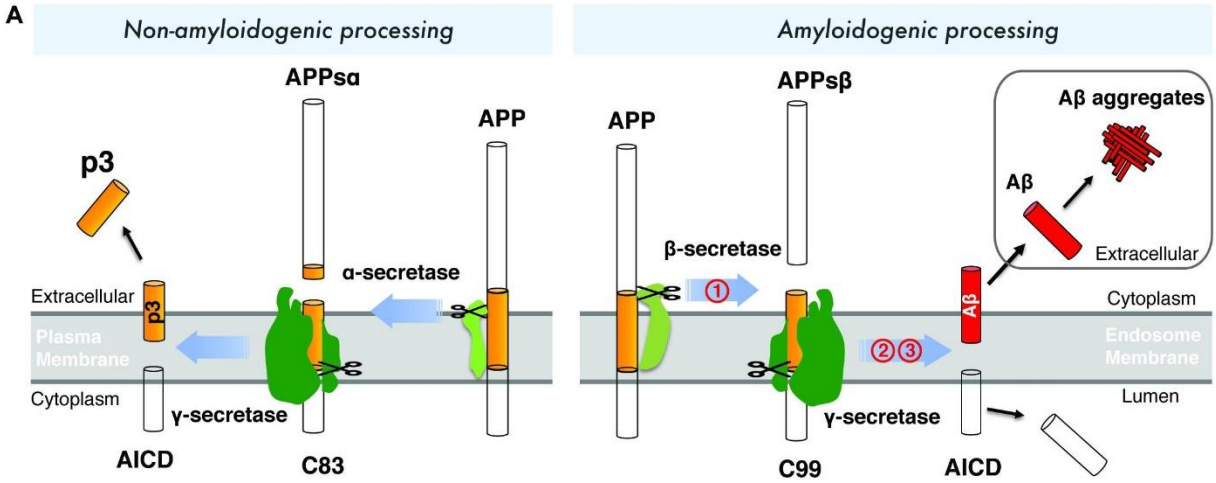

Figure 1. Visual depiction of the non-amyloidogenic and amyloidogenic pathways of APP processing. (Image taken from: Jing Zhao, Xinyue Liu, Weiming Xia, Yingkai Zhang and Chunyu Wang. Targeting Amyloidogenic Processing of APP in Alzheimer's Disease : in Research Journal Front. Mol. Neurosci., 04 August 2020)

APP-CTF is subsequently cleaved by γ-secretase to generate either a 3 kDa protein (p3, formed from APP-CTFα) or Aβ (formed from APP-CTFβ). Both processes release the APP intracellular domain (AICD) [12].

Depending on the initial cleavage site, one of two pathways is initiated. Cleavage performed by β-secretase, also known as β-site APP cleaving enzyme (BACE1), will result in C99 APP-CTFβ. This initiates the amyloidogenic pathway [12]. On the other hand, cleavage at the alpha site results in C83 APP-CTFα inhibiting the possibility of Aβ generation. For this

reason, α-secretase proteins are drug targets for treatment of AD. Their overexpression was shown to reduce Aβ generation of the cell [13]. There are multiple zinc dependent proteins from the disintegrin and metalloproteinase (ADAM) family capable of α-secretase activity. Some of these are ADAM9, ADAM10, TACE/ADAM17, MDC-9, and an aspartic protease BACE2 [8].

In addition to the non-amyloidogenic and amyloidogenic pathways, there are several non-canonical pathways through which APP can be processed. The APP C terminus can also be cleaved by caspases at Asp664 to yield C31 CTF, which has been implicated in neuronal apoptosis [14].

1.4. Amyloidogenic pathway

After cleavage by β-secretase the newly formed 99 amino acid (AA) long CTF is processed by γ-secretase. Subsequent ε-cleavage by γ-secretase creates the Aβ49 or Aβ48 fragments with the release of AICD that is known to regulate gene expression. The generated Aβ49/48 fragment is then further shortened by γ-secretase [12]. The first cleavage site after ε is marked as ζ, while the consequential ones are marked γ [15]. Depending on the initial fragment the final product is either Aβ40 (Aβ49→Aβ46→Aβ43→Aβ40) or Aβ42 (Aβ48→Aβ45→Aβ42). Due to errors in processing, some other fragment lengths are possible. Because of this, the length of Aβ fragments can vary from 38 to 43 residue long Aβ fragments [12].

Fragment formation is considered to play a crucial role in AD formation. This is because it was shown that a change in ratio between Aβ 40/42 can contribute to the onset of AD. Additionally, mutations that lead to early-onset AD shift the formation of Aβ to the longer 42 variant. Aβ42 is more hydrophilic and therefore has a higher tendency to bind to different protein structures [12]. Since γ-secretase is the protein responsible for fragment formation, it became the focus for understanding and curing AD.

1.5. γ-secretase

Protein from the family of intermembrane cleaving proteases have the proteolytic capability to cleave APP within its TM domain [10]. It is characterized as a high molecular weight complex consisting of four different subunits nicastrine (NIC), presenilin (PSEN) consisting of PSEN1 and 2, presenilin enhancer protein 2 (PEN2) and anterior pharynx-defective 1 (APH1) [16].

The first part of the complex to be identified was PSEN1. It was discovered through analysis of FAD patients linking a mutation on chromosome 14q24.3 with AD onset [17]. PSEN2 was identified in a similar fashion. Further analysis showed that PSEN 1 and 2 come together to form a complex with an aspartic active site. This site was later identified as the catalytic core of the γ-secretase complex [10]. Over time more than 150 mutations were identified (mainly in the PSEN1 domain). All seemed to increase the relative abundance of the more aggregate prone Aβ 42 fragment [18]. The PSEN complex is a 9TM domain heterodimer. Its active site is contained between TM6-TM7, with a proposed mechanism of docking occurring through TM6-TM9 [19]. PSEN also contains the PAL motif on TM9, which is essential for drug binding of γ-secretase modulators [20].

Several studies suggested that PSEN on its own lacks proteolytic activity, suggesting that additional protein components are required to form mature, stable PSEN heterodimers [10].

The first cofactor was isolated through coimmunoprecipitation with an anti-PSEN1 antibody. It was identified as NIC, a highly glycosylated 130 kDa type 1 transmembrane protein [16]. It acts as a scaffolding protein for γ-secretase interacting initially with APH1, followed by the incorporation of PSEN and PEN2. It has also been suggested that NIC can interact with APP to mediate its bonding with the PSEN subunit [21].

Screening in C. elegans identified two additional components, PEN2 and APH1 [10].

Aph-1 is a 29 kDa protein with seven TMs. Alongside NIC it plays a crucial role in the assembly process. Mutation of Gly122 to aspartic acid in humans results in a loss-of-function by hindering its association with the γ-secretase complex [22]. In humans, APH1 comes in three forms (APHaS, APH1aL, APH1b) encoded by two APH1 genes. Depending on the isoform, APP cleavage results in different lengths of Aβ. In mouse studies, γ-secretase complexes containing APH-1b tend to generate longer Aβ peptides relative to complexes containing APH-1a [16].

Isolated alongside APH1, PEN2 is the final component necessary for the function of γ-secretase. Down-regulation of PEN2 results in an accumulation of full-length PSEN1 and a reduction of PSEN1 fragments [16].

Besides Aβ, it was shown that γ-secretase is capable of processing more than 90 different type-I integral membrane proteins, the most important one being Notch [23]. The Notch receptor was shown to influence differentiation, proliferation, and apoptotic processes. For this reason, γ-secretase has received the name "the proteasome of the membrane". The many different functions of γ-secretase made the creation of Aβ-selective inhibitors challenging.

1.6. Criticism of the amyloid hypothesis

Aβ has dominated research on AD for decades, but it has failed to produce results. A common argument against the amyloid hypothesis is that plaques are found in the brains of many elderly people with normal cognition [24]. Furthermore, all drugs that successfully inhibit Aβ production by targeting γ-secretase complex have shown little to no effect, with some actually worsening cognitive decline [25].

1.7. Computational methods for protein visualization

Computational protein visualization is used to observe biological processes at a resolution that is not achievable by conventional methods. Programs run complex MD calculations to simulate the movement and action of atoms within a particular system. Currently, the most widely used program is Gromacs [26]. Protein visualization can be performed in two separate ways depending on the resolution needed. This is achieved by either using a more complex detailed system (AllAtom) or by using a rougher representation (Coarse Grained) [27,28]. In the AllAtom simulation every atom is represented by a single dot in the system, allowing higher accuracy in the time frame of up to 1 μs. On the other hand, Coarse Grained replaces a group of atoms with an imaginary single sphere severally reducing the complexity of the system. This makes it possible to run simulations that represent a longer period of time for up to 100 μs [27,28] (Fig 2).

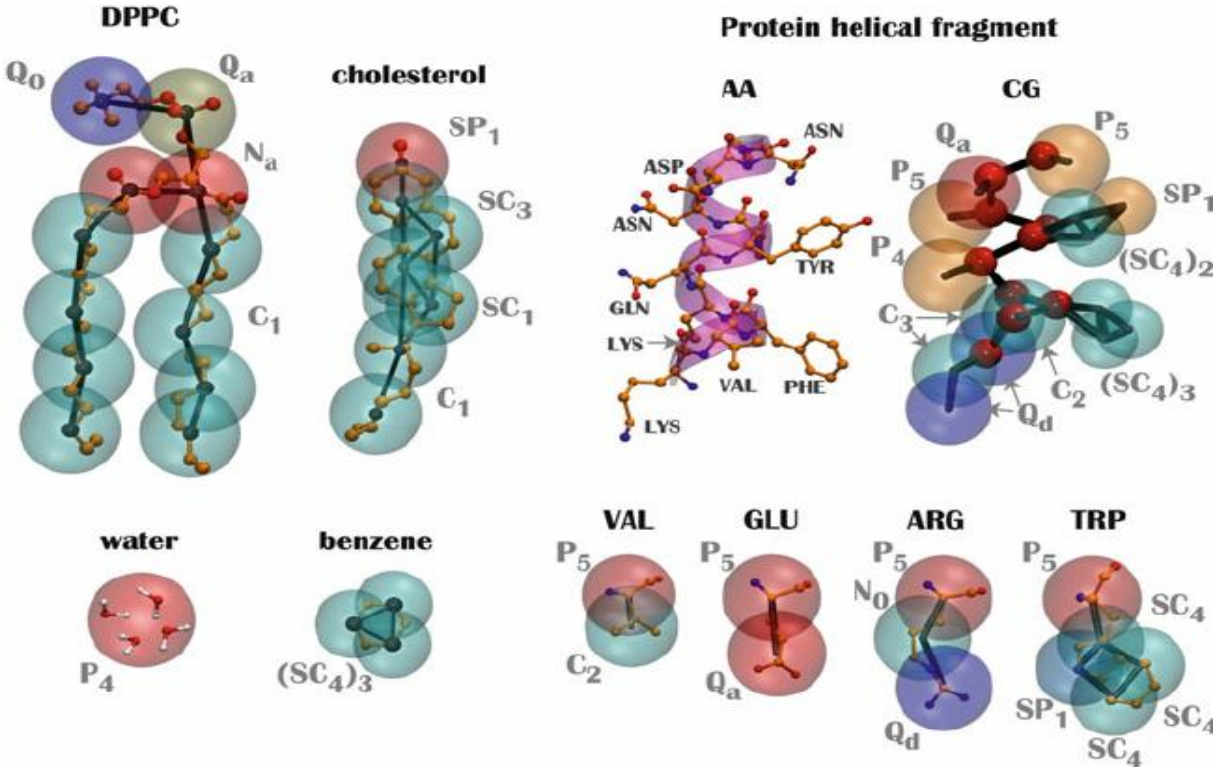

Figure 2. Difference between allatom and coarsegrained simulations. Atomistic structure represent what will be used in an AA simulation, while the transparent beads represent what will be used in a CG simulation. (image taken from: Xavier Periole, Siewert J Marrink. Xavier Periole Siewert J MarrinkThe Martini Coarse-Grained Force Field: in Methods in molecular biology (Clifton, N.J.) 924:533-65 · January 2013)

2. Objective

Since the protein's discovery, drugs that target γ-secretase have proven to be unsuccessful due to a lack of knowledge of the mechanism underlining AD formation. In this study we wanted to explore this mechanism, with the focus on the interactions with substrate. Additionally, we want to determine the role of NIC in the processing of Aβ.

3. Materials and methods

For MD simulations we used two different structures obtained by Cryo-EM NMR imaging: PDB ID 6IYC for γ-secretase and PDB ID 2LP1 for APP-CTFβ [29,30]. Structures were downloaded from the Protein Data Bank (PDB) and further modified using Chimera [31]. Protein orientation in a lipid bilayer was calculated using the Orientate Protein in Membrane online server (OPM) after which the pdb file was processed using Charmm-gui input generator [32,33]. Simulations were run using Gromacs MD program [26].

Since all the processes occur within the lipid bilayer a realistic approximation was used, hence all the simulations were performed in a cholesterol-rich membrane.

For analysis, a large array of programs and tools were used. VMD was used for visualization, calculating bond distances and polar interactions [34]. Next Chimera, Pymol and Avogadro were used for structural and electrostatic analysis. LibreOffice Calc. for charts and data visualization [31,35,36].
All simulations were performed using the supercomputer Bura [37].

3.1. All atom simulations

All atom simulations were performed using the charmm36 force field [38]. Compiling and preparation of the simulation was performed using Charmm-gui membrane builder, while for the equilibration and relaxation of the system, Gromacs was used [26,32].

The membrane composition used was (in number of molecules):
phosphatidylcholine (POPC), 152, 21%; phosphatidylethanolamine (POPE), 78, 11%; phosphatidic acid (POPA), 8, 1%; phosphatidylserine (POPS), 28, 4%; sphingomyelin (PSM), 42, 6%; phosphatidylinositol (POPI), 14, 2%; cholesterol (CHOL), 386, 55%.
For the rest of the details, I followed a protocol used by BioSFGroup [39].

3.2. Coarse Grained simulations

Coarse Grained simulations were performed using the martini2.2 force field. Compiling and preparation of the simulation were performed using Charmm-gui martini maker, while for the equilibration and relaxation of the system, Gromacs was used [26,32].

Membrane composition: 2.4 times the size, but same ratio of components.
For the rest of the details, I followed a protocol used by BioSFGroup [39]

3.3. Backward protocol

To perform certain type of analysis, frames from the CG simulations were transformed into All-atom. It was done using the Backward.py python script or the online alternative at Charm-gui [40].

VMD was used for frame extraction by including the "name BB" "name SC1-4", which in CG simulations limits the extraction of coordinates to just the protein. When converting anything other than the protein, additional

mapping files had to be downloaded.

The all-atom topology file necessary for the functioning of the script was prepared using Charmm-gui, and/or Gromacs in a combination with the charmm36 force field downloaded from the Charmm-gui website [26,32].

3.4. Simulating Aβ fragments

To represent the Aβ46 fragment, the substrate γ-secretase complex (PDB ID 6iyc) was used as an initial point of substrate generation [30]. After that, we started a 10 μs simulation. In that duration γ-secretase positioned Aβ49 at the active site where we then manually cleaved Aβ49 into the smaller Aβ46 using Chimera [31].

3.5. Modeling missing segments

Full length C99-βCTF-APP structures were built from NMR structures using modeler addon for Chimera (2LP1ref, modeler). The existing transmembrane section (AA 29 to 54) was positioned in cholesterol-mix-bilayer. Unstructured sections at the cytosolic end (AA 1 to 28) and the extracellular end (AA 55 to 99), were built as extended forms with no secondary structure presumptions. The same procedure was applied to Aβ N terminal end [41].

The NMR-obtained transmembrane section (AA 29-54) was positioned in lipid bilayer while its cytosolic (AA 55-99) and extracellular end (AA 1-28), were computationally modeled as extended forms. All modeled parts were modeled in an extended form as to not assume the secondary structure. For the Aβ fragment, only the extracellular end needed modeling.

4. Results

4.1. Interaction of C99-βCTF in membrane

Experimental data indicates that C99-βCTF can form dimers with itself [42]. We wanted to find out if such binding could occur between C99-βCTF and its derivatives. For this we used multiscale molecular dynamics. This was done by running coarse grained 10 μs simulations of the protein with the Aβ 49 and 46 fragments. Structures were derived from PDB and orientated in the system. Calculations started with the two molecules positioned 30 angstroms apart in a cholesterol-mix-bilayer.

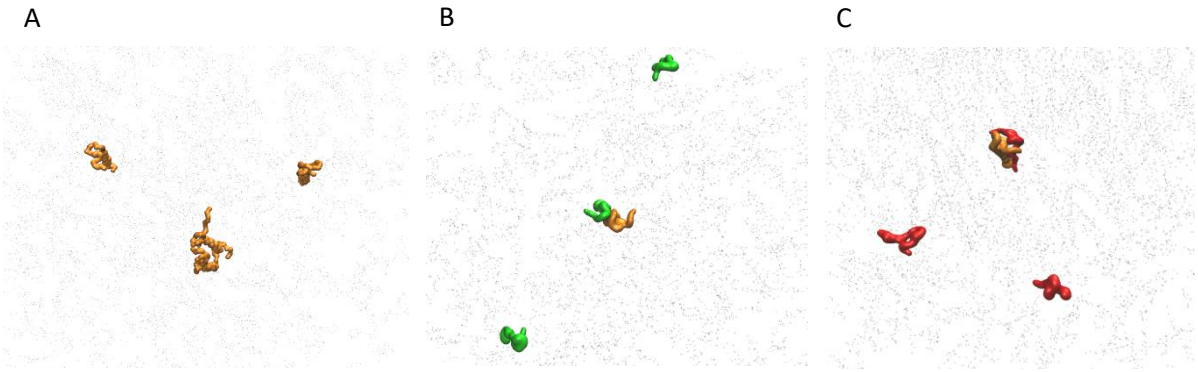

Figure 3. ***Binding of APP derived fragments in the cholesterol rich bilayer.*** *We used cryo-EM coordinates (PDB:2LP1). Images represent binding interactions after a 10 μs simulation. Visualization was preformed using the VMD program (A) 4 molecules of C99-βCFT represented as orange. (B) C99-βCFT represented as orange with 3 Aβ 49 molecules represented as green. (C)*

We found that if free, lipid-soluble fragments Aβ 49 and 46 encounter C99-βCTF, they can form stable dimers (Fig 3).

4.2. Docking of C99-βCTF

After confirming possible binding of C99-βCTF to different fragments we wanted to explore its binding to γ-secretase. This idea is an expansion of proposals that γ-secretase has an active site and a docking site allowing it to harbor two substrates at once [43].

The part of C99-βCTF with the strongest binding tendency is not visible in the original structure file [29]. This indicates that these parts of the protein have a high mobility, making them impossible to image. Because of that these structures are excluded from the initial 2LP1 structure (for C99-βCTF), 6IYC (for Aβ). To better represent biological processes, we needed a complete model of the structures. For this we used the modeler addon to build the missing structures (see methods for more information). C99-βCTF was placed 30 angstroms from Aβ on the protein side facing PSEN. Multiple molecular dynamics simulations were set to explore different impacts of C99-βCTF and to explore different interactions it achieved with the γ-secretase.

We found that C99-βCTF entered into an interaction with the enzyme, docking near the active site. The main AA identified as important for this result were PSEN LYKYR (AA 153-157) and NIC DPSKVPSENKD (AA 588 – 598) sequences (Fig 4).

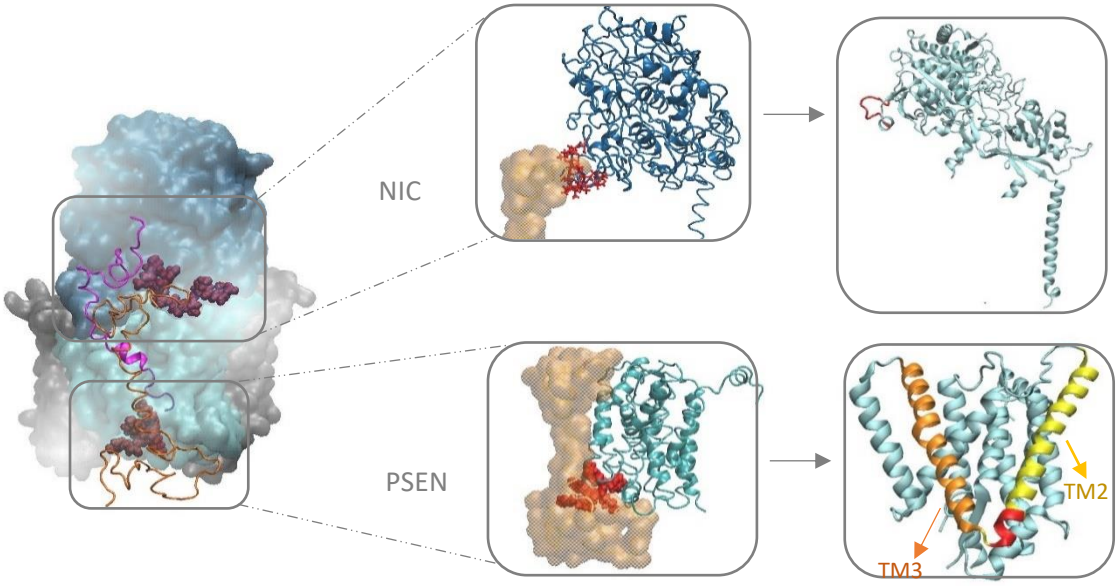

Figure 4. ***Visual depiction of C99-βCTF docking to the γ-secretase complex.*** *We used cryo-EM coordinates (PDB:2LP1). Images represent binding interactions after a 10 μs Coarse Grained simulation. Visualization was preformed using the VMD program. For a higher resolution, the structure was transformed to AllAtom using Backward.py. Representation are as follows: NIC blue, PSEN light blue, bound substrate magenta, free substrate orange, interactions with C99-βCTF red. Simulation resulted in the binding of C99-βCTF to the γ-secretase complex with main interactions at NIC and PSEN*

NIC first interacts with the N-terminal ectodomain, guiding the free C99-βCTF near the TM2-TM3 of PSEN. Resulted approaching allowed C99-βCTF to interact with PSEN. This caused a change in conformation of the C-terminal ectodomain and consequential binding to the loop that connects TM2-TM3. Additionally, PSEN Arg157 and Arg278 reacted to the overall global negative charge of the C99-βCTF ectodomain causing a change in the conformation of PSEN TM2, TM3, and cytosolic parts of TM6 and TM7. This interaction persisted for the duration of the simulation.

To see if the interaction is replicable, multiple simulations were run with the C99-βCTF in different positions, while still facing the PSEN side of the protein. Every time the result was the same with the C99-βCTF binding in the same way to γ-secretase (Fig 5).

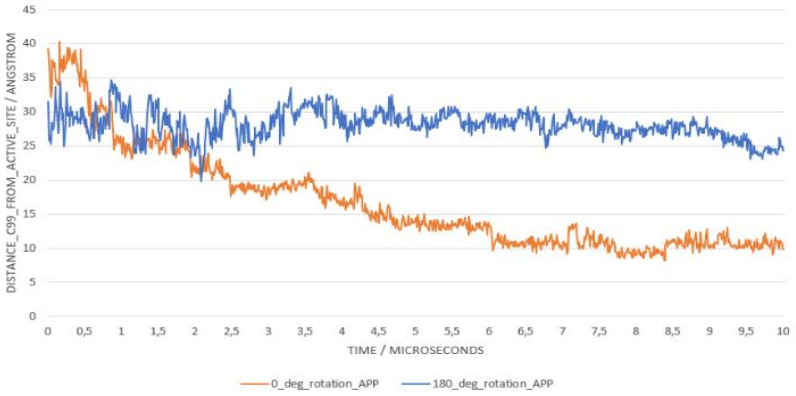

Figure 5. ***Effect of orientation on C99-βCTF binding to γ-secretase.*** *Plot depicts binding interactions after a 10 μs Coarse Grained simulation. Visualization was preformed using the VMD program. Representation are as follows: normal orange, 180 deg. blue. For approximation, distance between C99-βCTF GLY 38 backbone and substrate GLY 38 was compared. When rotated, C99-βCTF is unable to bind to the γ-secretase.*

To exclude the possibility of nonspecific binding we preformed docking with C99-βCTF rotated 180 degrees. This inhibited binding of C99-βCTF to γ-secretase excluding the possibility of nonspecific interaction.

4.3. Effect of nicastine on C99-βCTF and *γ*-secretase docking

There is an ongoing debate regarding whether NIC contributes to substrate docking [21]. To further explore its function, we limited the movement of NIC through the duration of the simulation, to prevent it from changing conformations and affecting the docking of C99-βCTF. The restrictions were introduced by modifying the rest.itp file [26]. To avoid artefacts, we preformed the simulation using the same layout and orientation as in the previous C99-βCTF docking experiment.

After the applied modification, binding of C99-βCTF was nonspecific. Interactions were always made with the part of the protein that was closest at the start of the simulation. Such behavior was not seen with a functional NIC (Fig 6).

Interestingly, if C99-βCTF binds close to the previous interaction site, the ectodomain migrates towards to the TM2-TM3 loop (Fig 6 D).

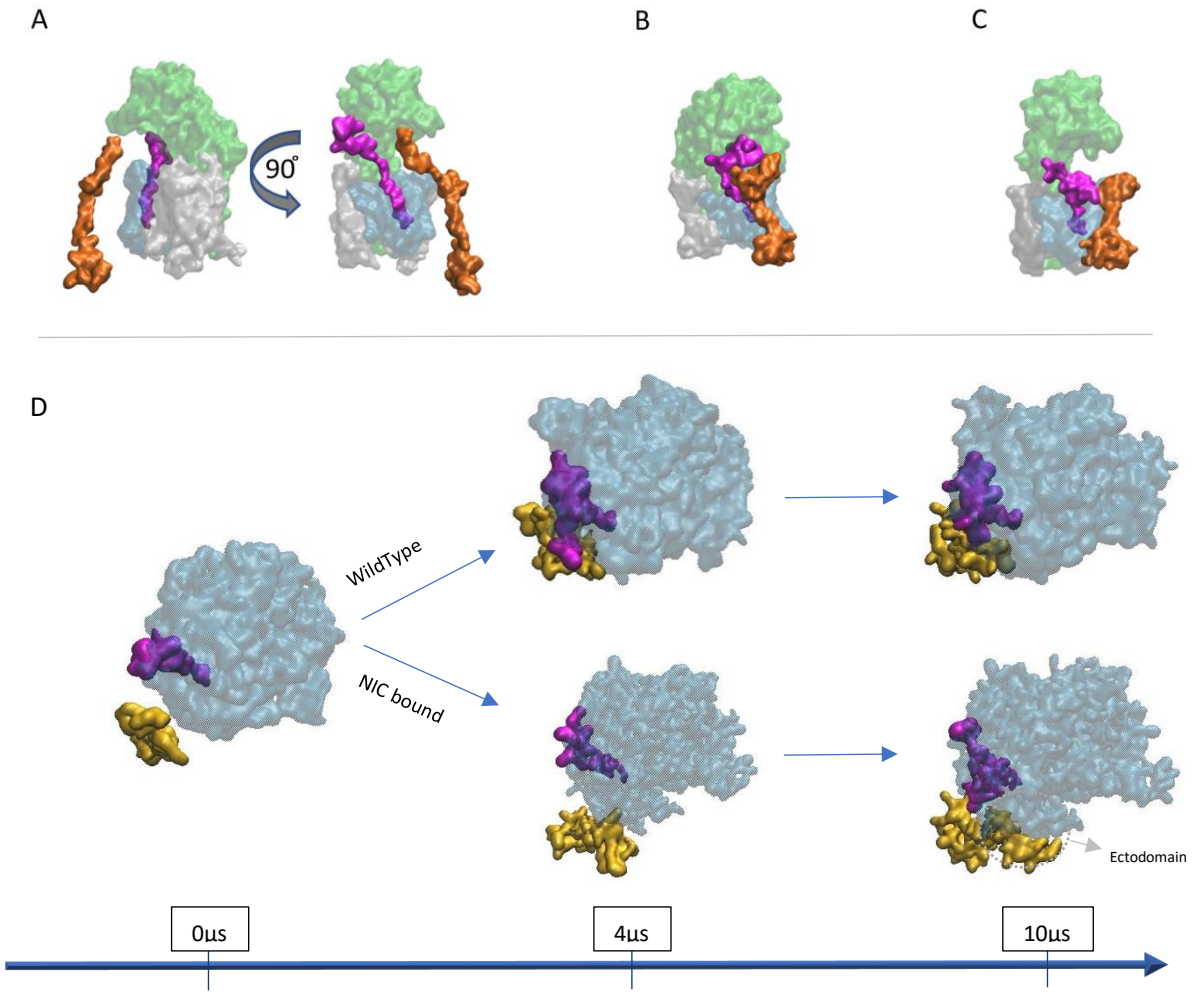

Figure 6. ***Binding of C99-βCTF to the γ-secretase complex depending on NIC activity.*** *We used cryo-EM coordinates (PDB:6IYC and 2LP1). Images represent binding interactions after a 10 µs Coarse Grained simulation. Visualization was preformed using the VMD program. (A-C) Representation are as follows: C99-βCTF orange, Aβ magenta, NIC green, PSEN blue. (A) First frame of the simulation. C99-βCTF was positioned 35 angstroms from the active site. (B) Docking of C99-βCTF with an active NIC after 10 µs. Interaction with NIC and PSEN stabilize the protein at the TM2-TM3 PSEN domain. (C) Docking of C99-βCTF with NIC in open position after 10 µs. Because of C99-βCTF proximity to the TM2-TM3, it is still capable to interact with PSEN, but the ectodomain remains bound to TM2 and TM6 of PSEN. (D) Top-down visualization of A-C. Representation are as follows: C99-βCTF light orange, Aβ magenta, γ-secretase blue.*

We then measured the change in distance between C99-βCTF and the active site. As an approximation, the distance between C99-βCTF Gly38 backbone and substrate Gly38 was compared (Fig 7).

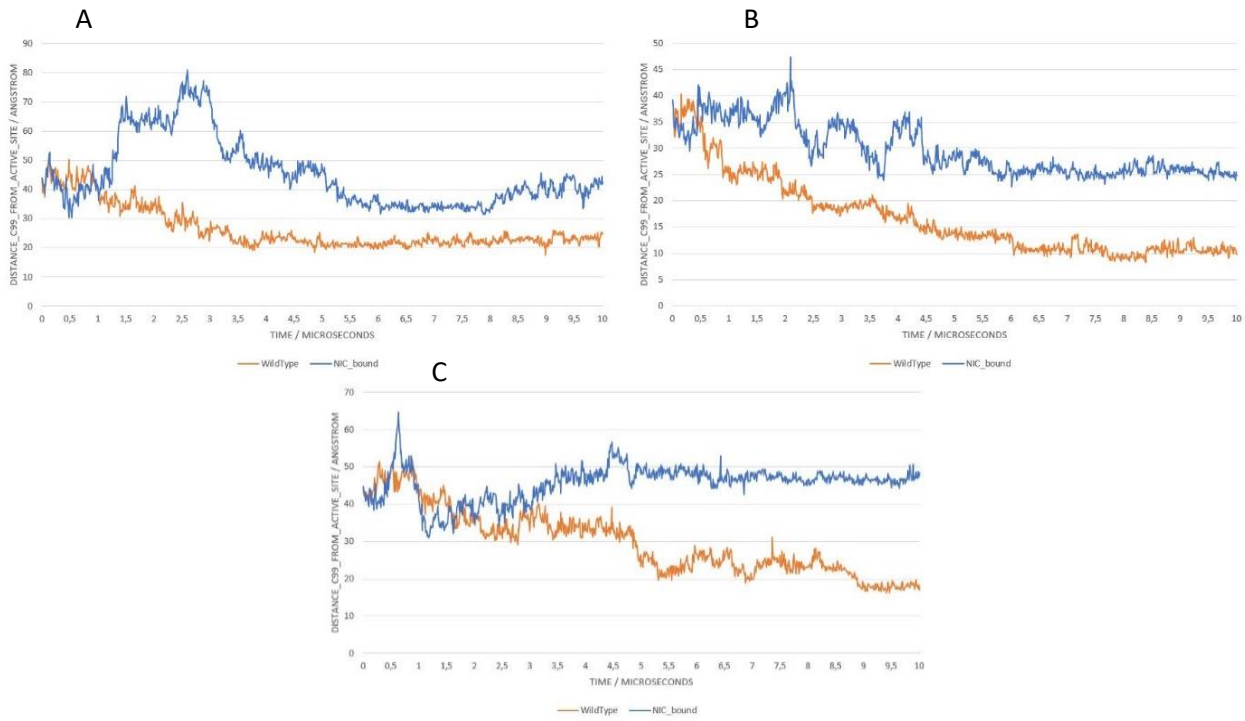

Figure 7. ***NIC effect on the binding of C99-βCTF.*** *(A-C) Binding interactions after a 10 μs Coarse Grained simulation. Visualization was preformed using the VMD program. Representation are as follows: NIC active orange, NIC restrained blue. For approximation, distance between C99-βCTF Gly38 backbone and substrate Gly38 was compared. In all simulations with NIC active C99-βCTF bound to the same distance from the active site. On the other hand, if NIC was bound in open position, C99-βCTF binds to the closest part of the protein resulting in apparent random distance change. (A) In the first frame of the simulation C99-βCTF is facing TM2 and TM6 of PSEN. (B) In the first frame of the simulation C99-βCTF is facing TM3 and TM4. (C) In the first frame of the simulation C99-βCTF is facing PSEN2.*

When NIC is active, similar binding can be observed. This interaction stabilizes 15-20 angstroms from the active site, where it stays until the end of the simulation. On the other hand, inactive NIC allows the binding of C99-βCTF to different parts of the γ-secretase complex. This results in a seemingly random change in protein distance from the active site.

4.4. **Substrate interaction and other NIC functions**

C99-βCTF was found to exhibit neurotoxic effect in high concentrations [14]. This combined with the cryo-EM studies that showed a large part of the bound substrate being accessible in the active site brought in to question possible interactions C99-βCTF could have with the substrate. Additionally,

there is no single conformation for the bond substrate that can be trapped by the cryo-EM studies [30]. Such lack of a specific conformation usually indicates the possibility for protein-protein interactions.

Further analysis of γ-secretase structure in simulations showed NIC ectodomain binding to PSEN and protecting the N-terminal domain of the substrate. The closing occurs before the free C99-βCTF diffuses towards the complex. This gave us the idea that NIC could possibly prevent the bound substrate from interacting with the free substrate.

We then positioned the free substrate in such a way that the closest part of the protein was the active site. Molecular dynamics simulations were again used, this time observing for a 6.4 μs timeframe.

As with previous simulations where we changed the orientation of C99-βCTF, we found that NIC was capable of inhibiting C99-βCTF docking (Fig 8 A-C). C99-βCTF was unable to approach γ-secretase complex and had minimal to no interactions with it.

To further explore the possible protective function of the NIC, we repeated the simulation with its ectodomain restrained in the open position. This time, C99-βCTF strongly bound to γ-secretase with the usual contacts on the 2TM-3TM loop. The ectodomain of C99-βCTF entered into polar interactions with the ectodomain of the bound substrate reaching up to 4H bonds (Fig 8 D). The new formed interaction resulted in the pulling of the bound substrate away from the active site (Fig 8 E). Distance from the active site was calculated by taking the average distance between the zeta site on the substrate and the active aspartates (Asp257 and Asp385)

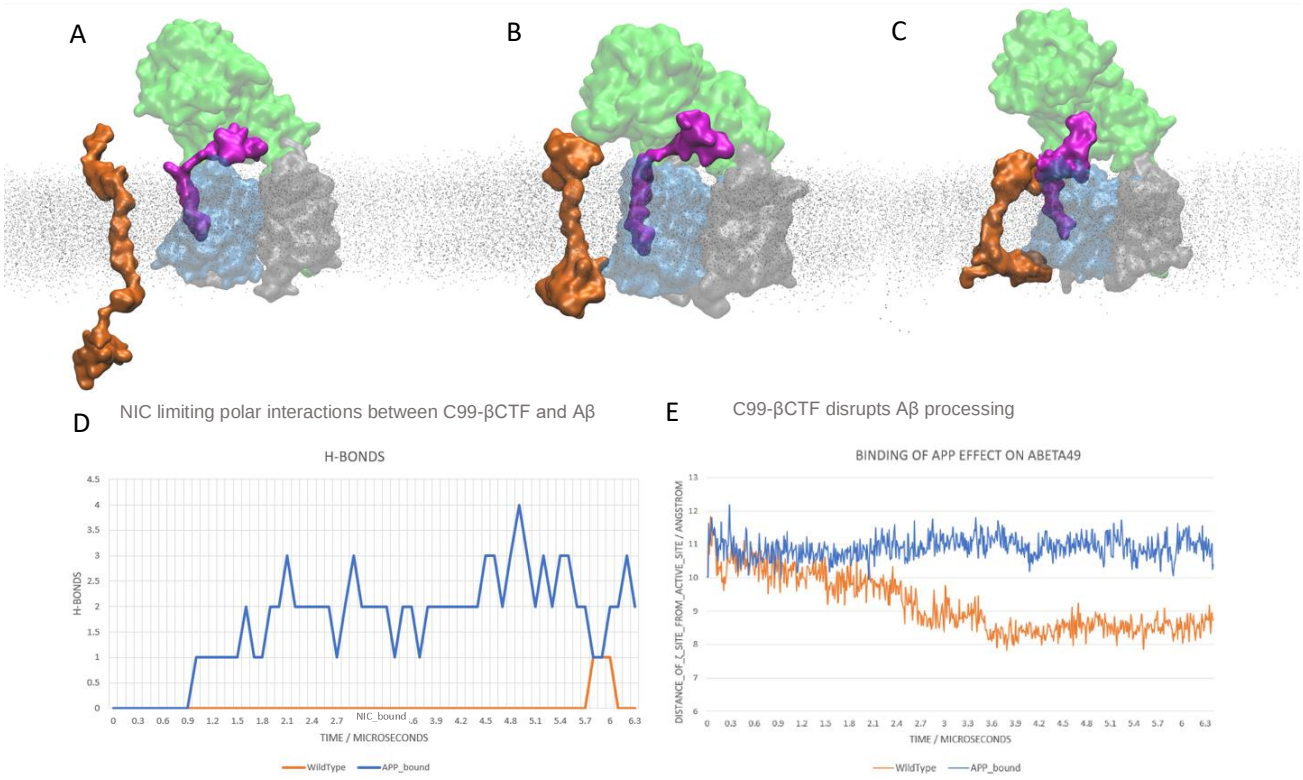

Figure 8. ***Disruption of the active site caused by substrate interaction and NIC role in Aβ protection.*** *(A-E) We used cryo-EM coordinates (PDB:6IYC and 2LP1). Images represent binding interactions after a 6.4 μs Coarse Grained simulation. Visualization was preformed using the VMD program. (A-C) Representation are as follows: C99-βCTF orange, Aβ magenta, NIC green, PSEN blue. Molecules are represented as quick surface (A) First frame of the simulation. C99-βCTF was positioned 13 angstroms from the active site. (B) Docking of C99-βCTF with an active NIC after 6.4 μs. NIC prevents docking and protects the N-terminal of the bound substrate. (C) With NIC bound in open position, C99-βCTF binds to the bound substrate. Image represents the system after 6.4 μs. (D) Numerical representation of the substrate-substrate interaction trough the simulation. Representation are as follows: NIC restrained blue, NIC active orange. (E) Disruption of the active site. Distance was measured from the active site aspartates to the ζ site. Representation are as follows: Normal system orange, Disrupted system by substrate-substrate binding blue. Binding of C99-βCTF caused a change in distance of the cleavage site from the active site.*

In real biological conditions, NIC exists in an active form and inhibits interactions with the substrate. Cryo-EM studies depict NIC in the open position, with the ectodomain of Aβ having multiple conformations. This indicates that NIC does not fully bind to the ectodomain. This differs from in-silico simulations where NIC creates a strong interaction with PSEN and APH-1 closing its structure within the first two μs of the simulation. The

probable reason being the inability to simulate glycosylation's that increase solubility. To avoid this artefact, we moved C99-βCTF closer to its binding site on PSEN (Fig 9 A). We again preformed a 10 μs molecular dynamics simulation. When bound, C99-βCTF was still capable of forming limited polar contact with the exposed section of the substrate (Fig 9 A-C).

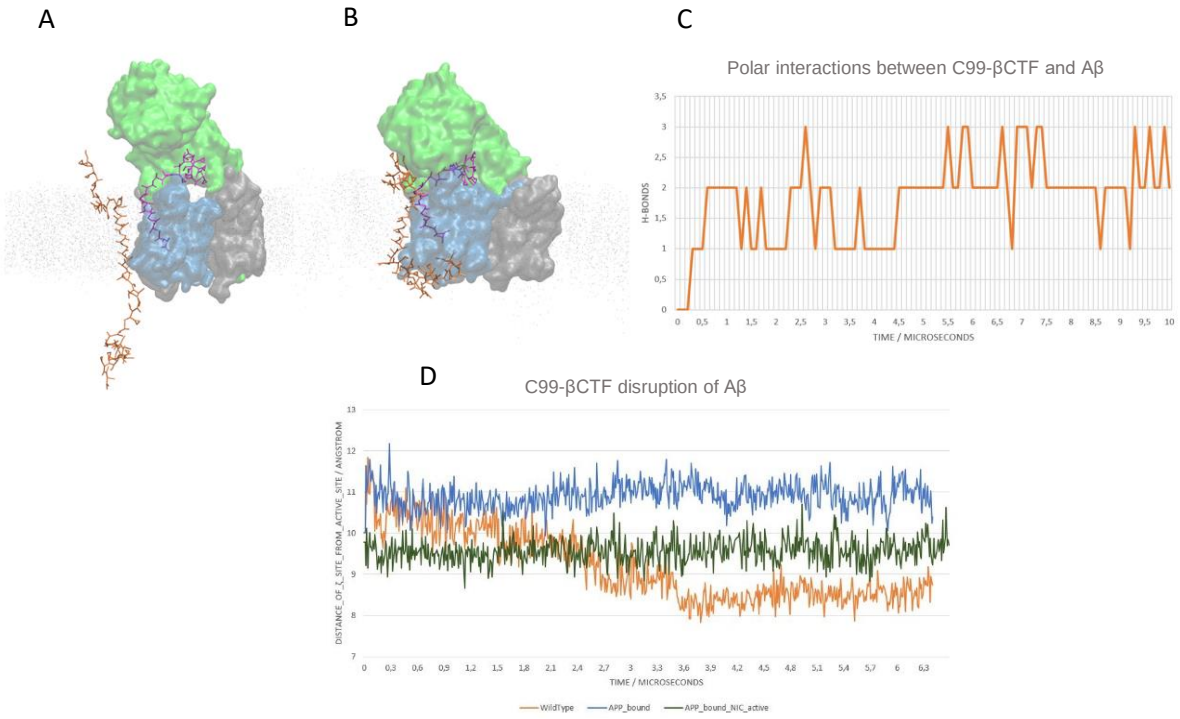

Figure 9. ***Disruption of the active site caused by substrate interaction.*** *We used cryo-EM coordinates (PDB:6IYC and 2LP1). Images represent binding interactions after a 10 μs Coarse Grained simulation. Visualization was preformed using the VMD program. NIC is active but the C99-βCTF is reduced to 9 angstroms from the active site. (A-B) Representation are as follows: C99-βCTF orange, Aβ magenta, NIC green, PSEN blue. NIC protects the N-terminal of the substrate but is not capable of inhibiting substrate interaction. (A) First frame of the simulation. C99-βCTF was positioned 9 angstroms from the active site. (B) Docking of C99-βCTF with an active NIC after 10 μs. (C) Numerical representation of the substrate-substrate interaction trough the simulation. (D) Disruption of the active site. Distance was measured from the active site aspartates to the ζ site. Representation are as follows: Normal system orange, NIC inactive with the system disrupted by substrate-substrate binding blue, NIC active with the system disrupted by substrate-substrate binding green. Active NIC can reduce effects of substrate interaction.*

We again saw an effect on the distance between the substrate and active site. When compared to the simulation with NIC ectodomain in the open position, we could see a diminished but persistent effect (Fig 8 D).

Lastly, we observed another chaperone-like effect of NIC ectodomain when it comes to substrate interaction. The firstly tightly bound ectodomain of substrate unraveled due to NIC activity in the course of the 10 μs simulation (Fig 9).

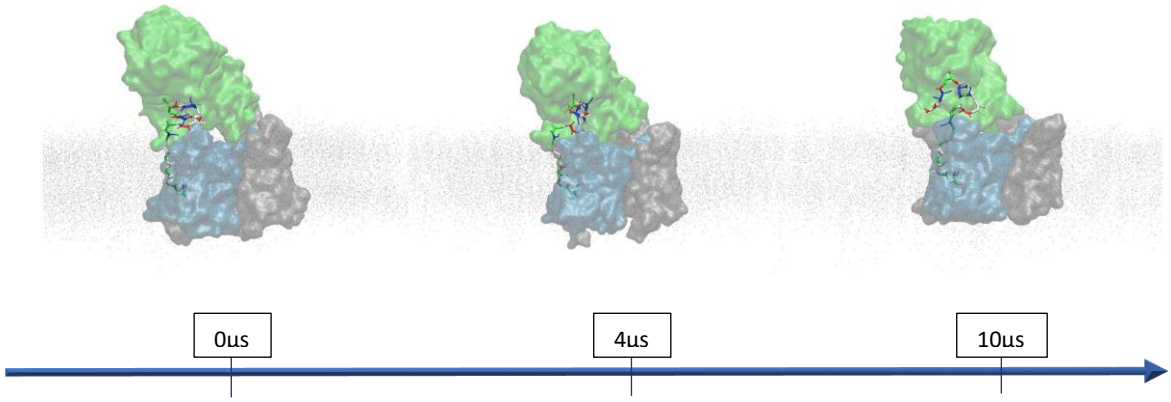

Figure 10. NIC unwinds N-terminal of Aβ We used cryo-EM coordinates (PDB:6IYC and 2LP1). Images represent binding interactions after a 10 μs Coarse Grained simulation. Visualization was preformed using the VMD program. Representation are as follows: Aβ based on amino acid polarity (white-hydrophobic, blue-positive charge, red-negative charge), NIC green, PSEN blue. NIC can unwind the N-terminal of Aβ.

5. Discussion

5.1. **The docking site and active site of the γ-secretase complex**

The existence of separate docking site and active site on the γ-secretase complex has long been disregarded. Nonetheless, some research indicates the possibility that two substrates simultaneously bind to γ-secretase [44]. This idea is in line with our results, with the binding of the second substrate always occurring in the same location on the PSEN subunit.

When binding to PSEN and NIC, the substrate forms a stable complex, always involving the same sequence. This happens regardless of the position docking occurs in. Such consistent behavior points to TM2-TM3 of PSEN as being a possible docking site. The idea of multiple substrates binding to γ-secretase is an attractive model that could explain some complex behavior observed in the pathogenesis of AD. Also, due to its proximity to the active site, substrate channeling could occur; shedding of the endodomain with epsilon cleavage would allow for the translocation of residual C terminal residues to the active site. This cleavage would be made accessible by a change in conformation of the bound substrate, possibly induced by BACE1. This differs from the traditional idea of the substrate entering the active site by penetrating the area between TM 6 and 9.

5.2. Nicastrine involvement in docking and processing of C99-βCTFs

NIC was considered to serve only as a scaffold for the formation of the γ-secretase complex. But recently it was observed that NIC has a larger contribution to substrate docking than previously thought, while also being capable of protecting the bound substrate [21,45]. Such functions were also observed in our results. By regulating its interactions with the protein, different kind of results could be achieved. Especially important when it comes to NIC was its capability to protect the bound substrate from protein interactions by sterically limiting bond formation. Also, as the first protein to bind with C99-βCTFs, regulation of NICs activity could change C99-βCTFs affinity for the γ-secretase complex and limit its interactions with PSEN.

Additionally, NIC can unfold the bound substrate. This chaperone-like ability could hint at a role of NIC in the mechanism Aβ oligomer formation, which is currently unclear in vivo [46].

5.3. Decrease in catalytic processing of γ-secretase pathogenesis of Alzheimer's disease

Analysis of mutations in PSEN revealed that they cause a decrease in catalytic capacity of γ-secretase [18]. Reduction of catalysis speed can lead to the accumulation of the longer more hydrophobic Aβ peptides. Interestingly, the same behavior was observed with γ-secretase inhibitors [25]. The exact mechanism by which this interaction could drive pathogenesis is still unknown.

The reason why the idea of a second substrate binding near the active site is so interesting is because it allows C99-βCTF to disrupt processing. Second binding of the free substrate could only occur in specific conditions. This is not possible in healthy biological systems, because enzymes are subsaturated allowing for the fastest cleavage of substrates. For double

substrate binding, a change of enzyme to substrate ratio would be needed. Such a change could be introduced by either diminishing active enzyme concentration, or by reduction of its catalytic capabilities. Because of this we propose that PSEN mutations and drug inhibition would allow for the binding of the second substrate [47]. The second substrate then further reduces catalysis speed by interacting with the bound amyloid protein. Furthermore, if C99-βCTF sufficiently increases the distance of Aβ from the active site, it could inactivate γ-secretase by disabling substrate-enzyme dissociation. This in turn causes a positive feedback loop, in which the increase in enzyme saturation further decreases the overall catalytic speed of γ-secretase. This could explain the exponential progression of the disease in the later stages of AD.

Beside the decrease in speed of catalysis, binding of the second substrate could also cause a shift in the cleavage of the bound substrate. In our simulations we have observed 1-2 angstrom shift in ζ cleavage that roughly corresponds to the 1.5 angstrom length of one amino acid. This could shift the processing of the substrate from the 49->46->43->40 pathway to the neurotoxic 48->45->42 pathway.

This also explains the observed difference in neurotoxicity of C83-APP-CTFα and C99-APP-CTFβ [14]. APP-CTFα has a shorter N-terminal ectodomain than APP-CTFβ. This would limit possible interactions with the Aβ substrate in the active site, preventing disruption of the processing.

Instead of γ-secretase inhibition, we propose drugs that can stabilize NIC in its closed position. Such drugs could inhibit the disruption in the processing of the bound substrate without reducing the speed of catalysis.

If the proposed mechanism is correct, we would like to point out that research made with oversaturation of the enzyme is potentially flawed. This is because such research would always imitate pathological conditions.

6. Conclusion

In this study we have presented the γ-secretase double substrate binding model of AD pathogenisis. We propose that gradual saturation of γ-secretase with its substrate can be the pathogenic process responsible for AD formation. This is caused by the ability of γ-secretase to bind to multiple substrates, which can then form stable interactions. The resulting interactions inhibit enzyme function by disrupting active site processing, causing a reduction in catalytic speed and the generation of longer, more hydrophilic Aβ42. To our knowledge, it is the only mechanism capable of explaining different pathogenic changes observed in biochemical, cellular, and clinical studies of AD. Additionally, we have provided further evidence for the extensive function NIC serves in γ-secretase.

7. Literature

1 What is Alzheimer's? Alzheimer's Disease and Dementia. https://alz.org/alzheimers-dementia/what-is-alzheimers (accessed 1 Jun2021).

2 Liu P-P, Xie Y, Meng X-Y, Kang J-S. History and progress of hypotheses and clinical trials for Alzheimer's disease. *Signal Transduction and Targeted Therapy* 2019; **4**: 1–22.

3 Alzheimer's Disease Fact Sheet. National Institute on Aging. http://www.nia.nih.gov/health/alzheimers-disease-fact-sheet (accessed 1 Jun2021).

4 AD in the Policy Agenda | Identify Alzheimer's disease. https://www.identifyalz.eu/en/home/social-impact.html (accessed 1 Jun2021).

5 Facts and Figures. Alzheimer's Disease and Dementia. https://www.alz.org/alzheimers-dementia/facts-figures (accessed 1 Jun2021).

6 Risk Factors. Alzheimer's Research & Prevention Foundation. https://alzheimersprevention.org/alzheimers-info/risk-factors/ (accessed 7 Jun2021).

7 Oxford AE, Stewart ES, Rohn TT. Clinical Trials in Alzheimer's Disease: A Hurdle in the Path of Remedy. *Int J Alzheimers Dis* 2020; **2020**. doi:10.1155/2020/5380346.

8 Chen G, Xu T, Yan Y, Zhou Y, Jiang Y, Melcher K *et al.* Amyloid β: structure, biology and structure-based therapeutic development. *Acta Pharmacol Sin* 2017; **38**: 1205–1235.

9 Viola KL, Klein WL. Amyloid β oligomers in Alzheimer's disease pathogenesis, treatment, and diagnosis. *Acta Neuropathol* 2015; **129**: 183–206.

10 Zhang X, Li Y, Xu H, Zhang Y. The γ-secretase complex: from structure to function. *Front Cell Neurosci* 2014; **8**. doi:10.3389/fncel.2014.00427.

11 Müller UC, Deller T, Korte M. Not just amyloid: physiological functions of the amyloid precursor protein family. *Nat Rev Neurosci* 2017; **18**: 281–298.

12 Zhang Y, Thompson R, Zhang H, Xu H. APP processing in Alzheimer's disease. *Molecular Brain* 2011; **4**: 3.

13 Lichtenthaler SF, Haass C. Amyloid at the cutting edge: activation of α-secretase prevents amyloidogenesis in an Alzheimer disease mouse model. *J Clin Invest* 2004; **113**: 1384–1387.

14 Nhan HS, Chiang K, Koo EH. The multifaceted nature of amyloid precursor protein and its proteolytic fragments: friends and foes. *Acta Neuropathol* 2015; **129**: 1–19.

15 Zhao G, Mao G, Tan J, Dong Y, Cui M-Z, Kim S-H *et al.* Identification of a new presenilin-dependent zeta-cleavage site within the transmembrane domain of amyloid precursor protein. *J Biol Chem* 2004; **279**: 50647–50650.

16 Zhang X, Li Y, Xu H, Zhang Y. The γ-secretase complex: from structure to function. *Front Cell Neurosci* 2014; **8**. doi:10.3389/fncel.2014.00427.

17 Clark RF, Hutton M, Fuldner M, Froelich S, Karran E, Talbot C *et al.* The structure of the presenilin 1 (S182) gene and identification of six novel mutations in early onset AD families. *Nature Genetics* 1995; **11**: 219–222.

18 Kelleher RJ, Shen J. Presenilin-1 mutations and Alzheimer's disease. *PNAS* 2017; **114**: 629–631.

19 Wolfe MS. Toward the structure of presenilin/γ-secretase and presenilin homologs. *Biochimica et Biophysica Acta (BBA) - Biomembranes* 2013; **1828**: 2886–2897.

20 Sato C, Takagi S, Tomita T, Iwatsubo T. The C-Terminal PAL Motif and Transmembrane Domain 9 of Presenilin 1 Are Involved in the Formation of the Catalytic Pore of the γ-Secretase. *J Neurosci* 2008; **28**: 6264–6271.

21 Shah S, Lee S-F, Tabuchi K, Hao Y-H, Yu C, LaPlant Q *et al.* Nicastrin Functions as a γ-Secretase-Substrate Receptor. *Cell* 2005; **122**: 435–447.

22 Gertsik N, Chiu D, Li Y. Complex Regulation of gamma-Secretase: from Obligatory to Modulatory Subunits. *Front Aging Neurosci* 2015; **6**. doi:10.3389/fnagi.2014.00342.

23 Wolfe MS. Structure and Function of the γ-Secretase Complex. *Biochemistry* 2019; **58**: 2953–2966.

24 Makin S. The amyloid hypothesis on trial. *Nature* 2018; **559**: S4–S7.

25 Penninkilampi R, Brothers HM, Eslick GD. Pharmacological Agents Targeting γ-Secretase Increase Risk of Cancer and Cognitive Decline in Alzheimer's Disease Patients: A Systematic Review and Meta-Analysis. *J Alzheimers Dis* 2016; **53**: 1395–1404.

26 GROMACS - Gromacs. https://www.gromacs.org/ (accessed 9 Jun2021).

27 Dove MT. An introduction to atomistic simulation methods. ; : 31.

28 Joshi SY, Deshmukh SA. A review of advancements in coarse-grained molecular dynamics simulations. *Molecular Simulation* 2020; **0**: 1–18.

29 Bank RPD. RCSB PDB - 2LP1: The solution NMR structure of the transmembrane C-terminal domain of the amyloid precursor protein (C99). https://www.rcsb.org/structure/2LP1 (accessed 9 Jun2021).

30 Bank RPD. RCSB PDB - 6IYC: Recognition of the Amyloid Precursor Protein by Human gamma-secretase. https://www.rcsb.org/structure/6IYC (accessed 9 Jun2021).

31 UCSF Chimera Home Page. https://www.cgl.ucsf.edu/chimera/ (accessed 9 Jun2021).

32 CHARMM-GUI. https://www.charmm-gui.org/?doc=input (accessed 9 Jun2021).

33 OPM. https://opm.phar.umich.edu/ppm_server (accessed 9 Jun2021).

34 VMD GRUPA. https://www.vmdgrupa.hr/ (accessed 9 Jun2021).

35 PyMOL | pymol.org. https://pymol.org/2/ (accessed 9 Jun2021).

36 Avogadro - Free cross-platform molecular editor - Avogadro. https://avogadro.cc/ (accessed 9 Jun2021).

37 Computing resources – Center for Advanced Computing and Modelling. https://cnrm.uniri.hr/bura/ (accessed 9 Jun2021).

38 CHARMM36 Lipid Force Field with Explicit Treatment of Long-Range Dispersion: Parametrization and Validation for Phosphatidylethanolamine, Phosphatidylglycerol, and Ether Lipids | Journal of Chemical Theory and Computation. https://pubs.acs.org/doi/10.1021/acs.jctc.0c01327 (accessed 9 Jun2021).

39 Research — BioSFGroup homepage. https://www.svedruziclab.com/research/ (accessed 9 Jun2021).

40 Resolution transformation. http://cgmartini.nl/index.php/tools2/resolution-transformation (accessed 9 Jun2021).

41 Sgro J-Y. MODELLER - II - Chimera GUI interface. ; : 20.

42 Isbert S, Wagner K, Eggert S, Schweitzer A, Multhaup G, Weggen S *et al.* APP dimer formation is initiated in the endoplasmic reticulum and differs between APP isoforms. *Cell Mol Life Sci* 2012; **69**: 1353–1375.

43 Kornilova AY, Bihel F, Das C, Wolfe MS. The initial substrate-binding site of γ-secretase is located on presenilin near the active site. *PNAS* 2005; **102**: 3230–3235.

44 Svedružić ŽM, Popović K, Smoljan I, Šendula-Jengić V. Modulation of γ-Secretase Activity by Multiple Enzyme-Substrate Interactions: Implications in Pathogenesis of Alzheimer's Disease. *PLOS ONE* 2012; **7**: e32293.

45 Nicastrin functions to sterically hinder γ-secretase–substrate interactions driven by substrate transmembrane domain | PNAS. https://www.pnas.org/content/113/5/E509 (accessed 9 Jun2021).

46 Sakono M, Zako T. Amyloid oligomers: formation and toxicity of Aβ oligomers. *The FEBS Journal* 2010; **277**: 1348–1358.

47 Szaruga M, Munteanu B, Lismont S, Veugelen S, Horré K, Mercken M *et al.* Alzheimer's-Causing Mutations Shift Aβ Length by Destabilizing γ-Secretase-Aβn Interactions. *Cell* 2017; **170**: 443-456.e14.